

Bi-allelic *DNAH8* Variants Lead to Multiple Morphological Abnormalities of the Sperm Flagella and Primary Male Infertility

Chunyu Liu,^{1,2,3,20} Haruhiko Miyata,^{4,20} Yang Gao,^{5,6,7,20} Yanwei Sha,^{8,9,20} Shuyan Tang,^{1,2,20} Zoulan Xu,^{4,10,20} Marjorie Whitfield,^{11,12,13} Catherine Patrat,^{11,12,13,14} Huan Wu,^{5,6,7} Emmanuel Dulioust,^{11,12,13,14} Shixiong Tian,^{1,2} Keisuke Shimada,⁴ Jiangshan Cong,^{1,2} Taichi Noda,⁴ Hang Li,^{5,6,7} Akane Morohoshi,^{4,15} Caroline Cazin,^{16,17,18} Zine-Eddine Kherraf,^{16,17} Christophe Arnoult,¹⁶ Li Jin,¹ Xiaojin He,^{5,6,7} Pierre F. Ray,^{16,17,21} Yunxia Cao,^{5,6,7,21} Aminata Touré,^{11,12,13,21} Feng Zhang,^{1,2,3,21,*} and Masahito Ikawa^{4,10,15,19,21,*}

Sperm malformation is a direct factor for male infertility. Multiple morphological abnormalities of the flagella (MMAF), a severe form of asthenoteratozoospermia, are characterized by immotile spermatozoa with malformed and/or absent flagella in the ejaculate. Previous studies indicated genetic heterogeneity in MMAF. To further define genetic factors underlying MMAF, we performed whole-exome sequencing in a cohort of 90 Chinese MMAF-affected men. Two cases (2.2%) were identified as carrying bi-allelic missense *DNAH8* variants, variants which were either absent or rare in the control human population and were predicted to be deleterious by multiple bioinformatic tools. Re-analysis of exome data from a second cohort of 167 MMAF-affected men from France, Iran, and North Africa permitted the identification of an additional male carrying a *DNAH8* homozygous frameshift variant. *DNAH8* encodes a dynein axonemal heavy-chain component that is expressed preferentially in the testis. Hematoxylin-eosin staining and electron microscopy analyses of the spermatozoa from men harboring bi-allelic *DNAH8* variants showed a highly aberrant morphology and ultrastructure of the sperm flagella. Immunofluorescence assays performed on the spermatozoa from men harboring bi-allelic *DNAH8* variants revealed the absent or markedly reduced staining of *DNAH8* and its associated protein DNAH17. *Dnah8*-knockout male mice also presented typical MMAF phenotypes and sterility. Interestingly, intracytoplasmic sperm injections using the spermatozoa from *Dnah8*-knockout male mice resulted in good pregnancy outcomes. Collectively, our experimental observations from humans and mice demonstrate that *DNAH8* is essential for sperm flagellar formation and that bi-allelic deleterious *DNAH8* variants lead to male infertility with MMAF.

Human infertility, defined as the inability to achieve a clinical pregnancy despite 12 months of regular and unprotected intercourse, has become a widespread health issue.¹ Multiple morphological abnormalities of the flagella (MMAF) are defined by the combination of absent, short, bent, coiled, and/or irregular-caliber flagella.² Previous genetic studies revealed a series of MMAF-associated genes in cases of primary infertility without primary ciliary dyskinesia (PCD; MIM: 244400) associated symptoms (reviewed by Touré et al.).^{3–14} However, these genetic findings account for approximately 35% to 60% of MMAF

cases,^{11,12} demonstrating the high genetic heterogeneity of this disorder and the necessity for further genetic explorations.

Cilia and flagella are hair-like organelles extending from the cell surface.^{15,16} Both contain an important core component, termed the axoneme, which is an evolutionarily conserved structure consisting of a highly ordered “9 + 2” arrangement of nine peripheral microtubule doublets and two central microtubules.¹⁷ A number of multi-protein complexes (including radial spokes, nexin-dynein regulatory complex, central complex, and dynein arms)

¹Obstetrics and Gynecology Hospital, NHC Key Laboratory of Reproduction Regulation (Shanghai Institute of Planned Parenthood Research), State Key Laboratory of Genetic Engineering at School of Life Sciences, Fudan University, Shanghai 200011, China; ²Shanghai Key Laboratory of Female Reproductive Endocrine Related Diseases, Shanghai 200011, China; ³State Key Laboratory of Reproductive Medicine, Center for Global Health, School of Public Health, Nanjing Medical University, Nanjing 211116, China; ⁴Research Institute for Microbial Diseases, Osaka University, Osaka 565-0871, Japan; ⁵Reproductive Medicine Center, Department of Obstetrics and Gynecology, The First Affiliated Hospital of Anhui Medical University, Hefei 230022, China; ⁶NHC Key Laboratory of Study on Abnormal Gametes and Reproductive Tract, Anhui Medical University, Hefei 230032, China; ⁷Key Laboratory of Population Health Across Life Cycle, Anhui Medical University, Ministry of Education of the People's Republic of China, Hefei 230032, China; ⁸Department of Andrology, United Diagnostic and Research Center for Clinical Genetics, School of Public Health & Women and Children's Hospital, Xiamen University, Xiamen 361005, Fujian, China; ⁹State Key Laboratory of Molecular Vaccinology and Molecular Diagnostics & Center for Molecular Imaging and Translational Medicine, School of Public Health, Xiamen University, Xiamen 361102, China; ¹⁰Graduate School of Pharmaceutical Sciences, Osaka University, Osaka 565-0871, Japan; ¹¹INSERM U1016, Institut Cochin, Paris 75014, France; ¹²Centre National de la Recherche Scientifique UMR8104, Paris 75014, France; ¹³Faculté de Médecine, Université de Paris, Paris 75014, France; ¹⁴Laboratoire d'Histologie Embryologie—Biologie de la Reproduction—CECOS Groupe Hospitalier Universitaire Paris Centre, Assistance Publique-Hôpitaux de Paris, Paris 75014, France; ¹⁵Graduate School of Medicine, Osaka University, Osaka 565-0871, Japan; ¹⁶Team Genetics Epigenetics and Therapies of Infertility, Institute for Advanced Biosciences, Grenoble Alpes University (UGA), INSERM U1209, Centre National de la Recherche Scientifique UMR 5309, Grenoble 38000, France; ¹⁷UM de génétique de l'infertilité et de diagnostic pré-implantatoire (GI-DPI), Centre Hospitalier Universitaire Grenoble Alpes (CHUGA), Grenoble 38000, France; ¹⁸Service de Génétique, Laboratoire Eurofins Biomnis, Lyon, France; ¹⁹Institute of Medical Science, University of Tokyo, Tokyo 108-8639, Japan

²⁰These authors contributed equally to this work

²¹These authors contributed equally to this work

*Correspondence: zhangfeng@fudan.edu.cn (F.Z.), ikawa@biken.osaka-u.ac.jp (M.I.)

<https://doi.org/10.1016/j.ajhg.2020.06.004>

© 2020 American Society of Human Genetics.

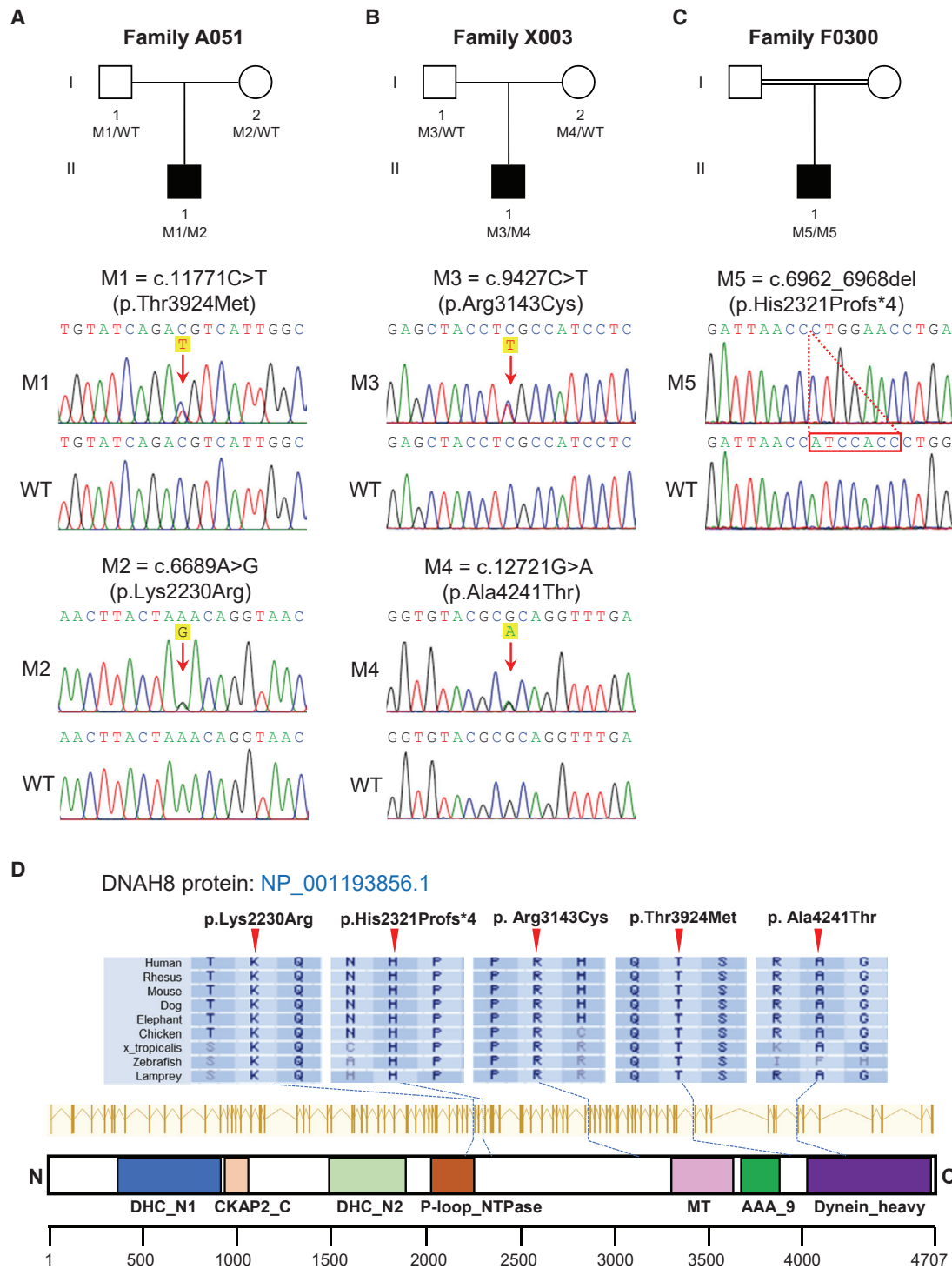


Figure 1. Identification of Bi-allelic *DNAH8* Variants in Men with MMAF

(A–C) The pedigrees of three families affected by *DNAH8* variants. The NCBI reference sequence number for *DNAH8* transcript is NM_001206927.2. Sanger sequencing results are shown below the pedigrees. The variant positions are indicated by red arrows or a dashed box. WT, wild type.

(D) Variant locations and phylogenetic conservation of the mutated residues in *DNAH8* protein. The NCBI reference sequence number for *DNAH8* protein is NP_001193856.1. Colored squares denote different domains according to the NCBI browser. DHC_N1—dynein heavy chain, N-terminal region 1; CKAP2_C—cytoskeleton-associated protein 2 C terminus; DHC_N2—dynein heavy chain, N-terminal region 2; P-loop_NTPase—P-loop containing nucleoside triphosphate hydrolases; MT—microtubule-binding stalk of dynein motor; AAA_9—ATP-binding dynein motor region D5; Dynein_heavy—dynein heavy chain and region D6 of dynein motor.

Table 1. Bi-allelic *DNAH8* Variants Identified in MMAF-affected Men

	Subject A051		Subject X003		Subject F0300
cDNA alteration	c.11771C>T	c.6689A>G	c.9427C>T	c.12721G>A	c.6962_6968del
Variant allele	heterozygous	heterozygous	heterozygous	heterozygous	homozygous
Protein alteration	p.Thr3924Met	p.Lys2230Arg	p.Arg3143Cys	p.Ala4241Thr	p.His2321Profs*4
Variant type	missense	missense	missense	missense	frameshift
Allele Frequency in Human Population					
1000 Genomes	0	0	0	0	0
gnomAD (v3)	0.006729	0	0.0004677	0.0001187	0
Function Prediction					
SIFT	damaging	damaging	damaging	damaging	NA
PolyPhen-2	damaging	damaging	damaging	damaging	NA
MutationTaster	damaging	damaging	damaging	damaging	damaging
NCBI reference sequence number of <i>DNAH8</i> is NM_001206927.2. NA, not applicable.					

constitute the major components of the axoneme.¹⁸ Among the complexes, the outer and inner dynein arms (ODAs and IDAs, respectively) play an important role in the beating of cilia and flagella through ATP hydrolysis.¹⁹ Previous studies have revealed that mutations in IDA and ODA protein complexes cause several ciliopathies and male infertility. In particular, the deficiency of *DNAH1* (MIM: 603332), which encodes an important component of the IDA heavy chain, leads to isolated male infertility with MMAF.² Importantly, recent studies reported that mutations in *DNAH17* (MIM: 610063; encoding a sperm-specific ODA heavy-chain component) also cause isolated male infertility due to asthenoteratozoospermia.^{13,20} These

findings suggest the potential involvement of other components of dynein arms in male infertility and sperm flagellar malformations.

Here, two distinct MMAF cohorts were analyzed. The first cohort comprised 90 Chinese MMAF-affected men enrolled from the First Affiliated Hospital of Anhui Medical University and the Women and Children's Hospital of Xiamen University in China. The second cohort comprised 167 individuals with MMAF, including 83 men from North Africa (Algeria, Libya, and Tunisia; enrolled at the Clinique des Jasmins in Tunis), 52 men recruited at the Royan Institute (Reproductive Biomedicine Research Center) in Iran, and 32 men recruited in France (mainly at the

Table 2. Semen Characteristics and Sperm Flagellar Morphology of Men Carrying Bi-allelic *DNAH8* Variants

	Subject A051	Subject X003	Subject F0300	Reference Values
Semen Parameters				
Semen volume (mL)	2.2	3.2	7.1	>1.5
Sperm concentration (10 ⁶ /mL)	39.1	42.7	13.6*	>15.0
Total sperm count (10 ⁶)	86.0	136.7	96.6	>39.0
Motility (%)	4.0*	2.7*	8.0*	>40.0
Progressive motility (%)	1.3*	1.5*	4.0*	>32.0
Sperm Flagellar Morphology				
Absent flagella (%)	2.0	2.5	4.0	<5.0
Short flagella (%)	7.1*	9.0*	8.0*	<1.0
Coiled flagella (%)	57.1*	32.0*	33.0*	<17.0
Angulation (%)	0.5	6.0	19.0*	<13.0
Irregular caliber (%)	1.0	26.0*	8.0*	<2.0
Normal flagella (%)	32.3	24.5	28.0	>23.0
Lower and upper reference limits are shown according to the World Health Organization standards ⁴⁶ and the distribution ranges of morphologically abnormal spermatozoa observed in fertile individuals. ⁴⁷ *Abnormal values.				

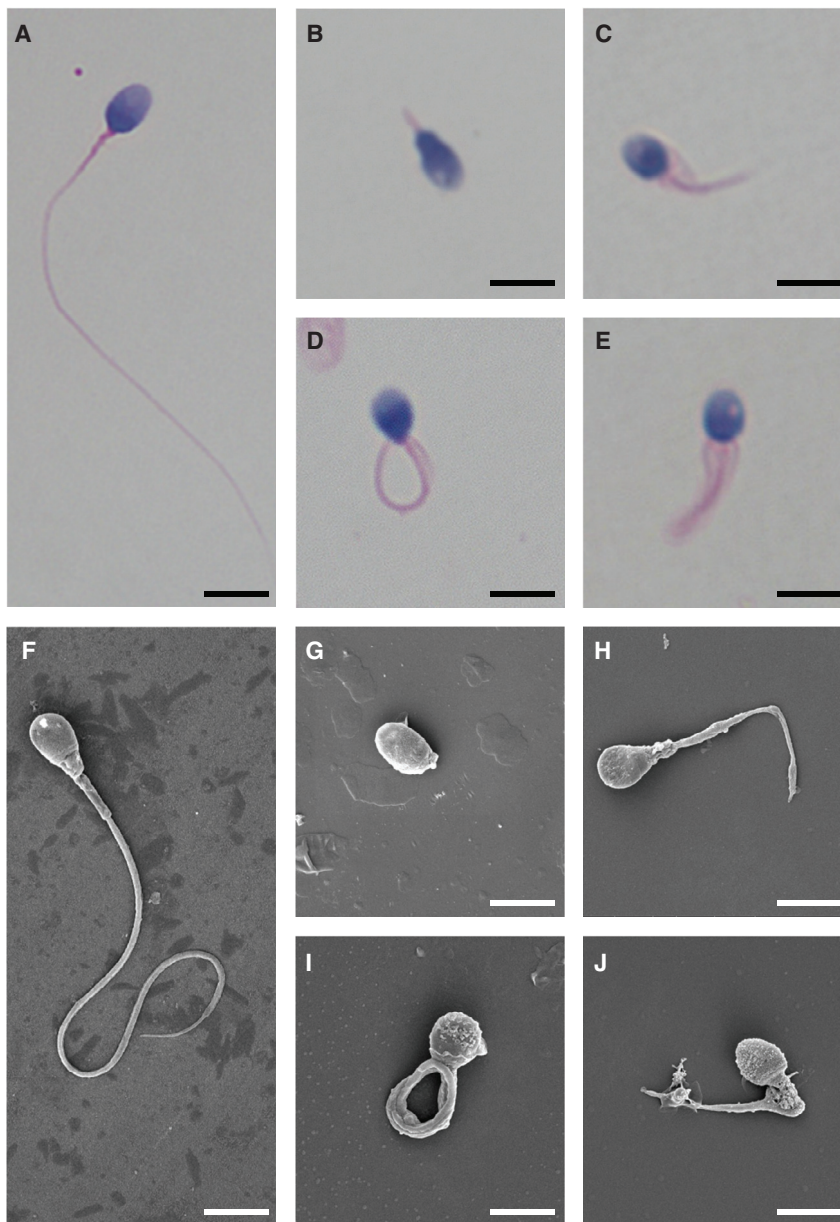


Figure 2. Morphology of the Spermatozoa from Men Harboring Bi-allelic *DNAH8* Variants

(A) Normal morphology of the spermatozoon from a healthy control male evident under light microscopy. Scale bars: 5 μ m.

(B–E) Most spermatozoa from men harboring bi-allelic *DNAH8* variants presented MMAF phenotypes, including absent (B), short (C), coiled (D), and irregular-caliber flagella (E). The data of subject A051 as an example.

(F) Normal morphology of the spermatozoon from a healthy control male as revealed by scanning electronic microscopy.

(G–J) The MMAF phenotypes, including absent (G), short (H), coiled (I), irregular-caliber flagella (J), were clearly revealed in the spermatozoa from subject A051 harboring bi-allelic *DNAH8* variants.

(p.Arg3143Cys) plus c.12721G>A (p.Ala4241Thr) in subject X003 (II-1 in Figure 1B). Subsequent Sanger sequencing confirmed that these bi-allelic *DNAH8* variants were inherited from heterozygous parental carriers (Figures 1A and 1B; Table S1). All of the *DNAH8* variants were either absent or rare in the human genome datasets archived in the 1000 Genomes Project and gnomAD databases. These *DNAH8* variants were also predicted to be damaging through the use of the PolyPhen-2, SIFT, and MutationTaster tools (Table 1).

WES analysis of the 167 MMAF-affected men from the second cohort identified an additional case in an individual of Moroccan ancestry (Figure 1C). This MMAF-affected subject F0300 (II-1 in Figure 1C) harbored

a homozygous frameshift variant (c.6962_6968del [p.His2321Profs*4]) that produced a frameshift and premature stop codon in *DNAH8*. No DNA was available from family members of subject F0300. His brother was reported to be infertile, although no further investigation could be performed. We note that his parents are consanguineous, thus strongly supporting the likelihood that this *DNAH8* frameshift variant was also transmitted under a recessive mode of inheritance.

Importantly, the residues in *DNAH8* affected by these aforementioned variants are all highly conserved across species (Figure 1D). Furthermore, no bi-allelic deleterious variants in previously described MMAF- or PCD-associated genes were observed in the three men with bi-allelic *DNAH8* variants. These findings further suggest that the infertility phenotypes were likely caused by the identified bi-allelic *DNAH8* variants.

Reproductive Department of the Cochin Hospital in Paris). The clinical phenotypes of the affected individuals are summarized in the Supplemental Note (see Supplemental Information). Informed consent was obtained from all subjects participating in the study. The study regarding the cohorts was approved by the institutional review boards at all of the participating institutes.

To investigate the unknown genetic factors involved in human MMAF, we performed whole-exome sequencing (WES) analyses in the first cohort of 90 Chinese men with MMAF. After applying stringent bioinformatic analyses according to our previously described protocol,⁴ we identified two men (2.2%) harboring bi-allelic missense variants in *DNAH8* (MIM: 603337; NCBI: NM_001206927.2). The *DNAH8*-mutated alleles were c.11771C>T (p.Thr3924Met) plus c.6689A>G (p.Lys2230Arg) in subject A051 (II-1 in Figure 1A) and c.9427C>T

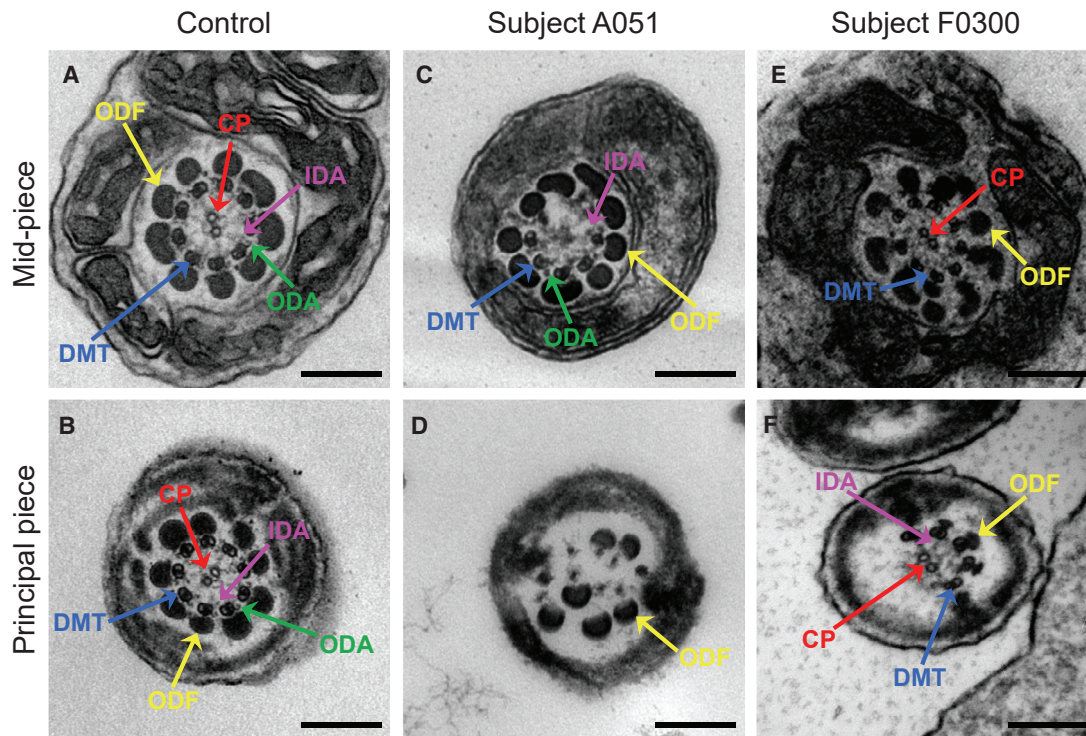


Figure 3. TEM Analyses of Sperm Cells from Men Harboring Bi-allelic *DNAH8* Variants

(A and B) Cross-sections of the mid-piece (A) and principal piece (B) of the sperm flagella in a control individual show the typical “9 + 2” microtubule structure, including nine pairs of peripheral microtubule doublets (DMT; blue arrows), nine outer dense fibers (ODF; yellow arrows), and the central pair of microtubules (CP; red arrows). The outer dynein arms (ODA; green arrows) and inner dynein arms (IDA; pink arrows) are also visible. Scale bars: 200 μ m.

(C–F) In the spermatozoa from men harboring bi-allelic *DNAH8* variants, various axonemal anomalies can be observed, including the lack of CP (C) or DMT (D). Misarranged (D) or supernumerary ODFs (E) were also observed. ODAs were disassembled or absent in the samples from men carrying bi-allelic *DNAH8* variants (C–F).

DNAH8 contains 92 exons and encodes a predicted 4,707-amino-acid protein (NCBI: NP_001193856.1; UniProt: A0A075B6F3). The *DNAH8* protein is preferentially expressed in the human testis, according to the Human Protein Atlas. Our reverse transcription polymerase chain reaction (RT-PCR) assays also indicated that mouse *Dnah8* is predominantly expressed in the testis (Figure S1A). Furthermore, the expression of mouse *Dnah8* mRNA in the testis began at 14 days after birth, corresponding to the pachytene stage (Figure S1B).

Semen parameters of men harboring bi-allelic *DNAH8* variants were analyzed in the source laboratories according to World Health Organization guidelines.²¹ Sperm motility and progressive motility in the men harboring bi-allelic *DNAH8* variants were dramatically lower than the normal reference values (Table 2). Hematoxylin-eosin (H&E) staining and scanning electron microscopy examination were performed to assess sperm morphology. Approximately 70% of the immotile spermatozoa displayed abnormal flagella, including absent, short, and coiled flagella, angulation, and irregular caliber (Figure 2 and Table 2).

Various ultrastructural defects were revealed by transmission electron microscopy (TEM) in the sperm flagella from men harboring bi-allelic *DNAH8* variants. The

typical “9 + 2” microtubule structure was observed in the spermatozoa from control men (Figure 3). However, a dramatic disorganization in axonemal or peri-axonemal structures (including disorganized peripheral microtubule doublets and outer dense fibers, missing or disassembled ODAs, and absent central pairs) was detected in the spermatozoa from men harboring bi-allelic *DNAH8* variants (Figure 3). Quantification conducted on transverse sections of the sperm flagella indicated higher rates of abnormal flagellar ultrastructure in men harboring bi-allelic *DNAH8* variants than those in the normal control (Table S2).

To further investigate the pathogenicity of bi-allelic *DNAH8* variants, we analyzed the levels of *DNAH8* mRNA and *DNAH8* protein using RT-PCR (Table S3) and immunofluorescence assays, respectively. The abundance of *DNAH8* mRNA in the sperm from subject A051, who harbored bi-allelic *DNAH8* variants, was significantly reduced when compared to the normal control (Figure S2). As for the protein level, in the normal control man, *DNAH8* immunostaining was concentrated along the mid-piece and principal piece of the sperm flagella (Figure S3). This observation in humans is consistent with previous evidence in wild-type male mice.²² In contrast, *DNAH8* immunostaining was almost absent in

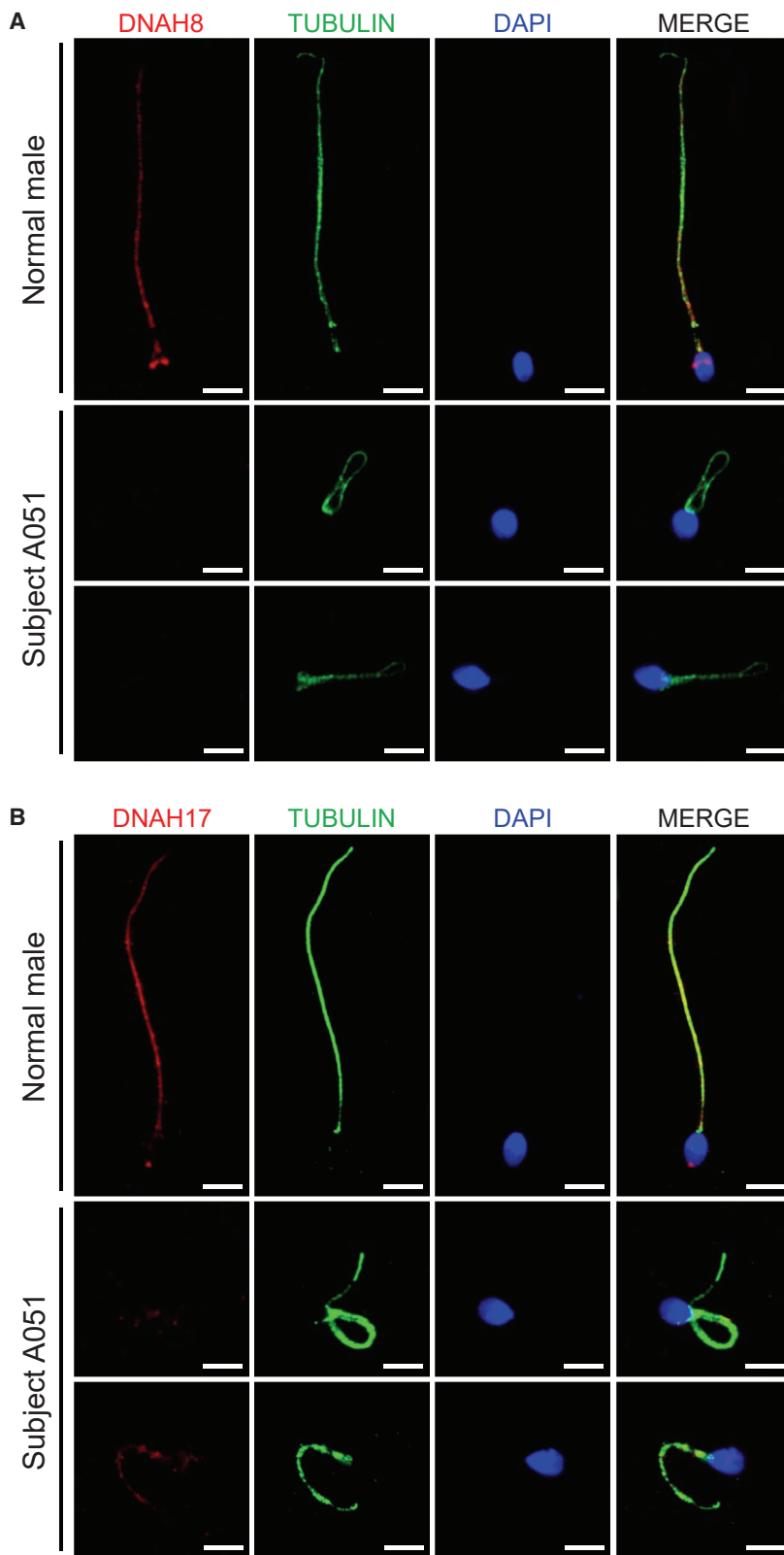


Figure 4. Localization of DNAH8 and Associated Protein DNAH17 in the Spermatozoa from Men Harboring Bi-allelic *DNAH8* Variants
 (A) Immunofluorescence staining of the spermatozoa from a normal control male and subjects carrying bi-allelic *DNAH8* variants. Anti-DNAH8 (red) and anti- α -tubulin (green) antibodies were used. Spermatozoa were counterstained with 4',6-diamidino-2-phenylindole as a marker of the cell nucleus. In the fertile control male, DNAH8 immunostaining (red) concentrated along the sperm flagella, but this signal was almost absent from the sperm flagella from subjects harboring bi-allelic *DNAH8* variants. The data of subject A051 are provided to illustrate the typical staining observed in the *DNAH8*-associated cases. Scale bars: 5 μ m.
 (B) DNAH17 immunostaining is affected in the spermatozoa from men harboring bi-allelic *DNAH8* variants. The spermatozoa were stained with anti-DNAH17 (red) and anti- α -tubulin (green) antibodies. DNAH17 staining mainly localized along the sperm flagella from a control male, while being evidently reduced in the spermatozoa from subject A051. Scale bars: 5 μ m.

of DNAH17 was dramatically reduced in the spermatozoa from men harboring bi-allelic *DNAH8* variants (Figure 4B and Figure S3B).

DNAH8 is highly conserved among different species during evolution. Consistent with the human data available from the Human Protein Atlas, the murine ortholog *Dnah8* is also preferentially expressed in the testis, as per our RT-PCR assays conducted in a set of various mouse tissues (Figure S1, Table S4). To further investigate the role of mouse *Dnah8* in sperm flagellar formation, we generated *Dnah8*-knockout (KO; *Dnah8*^{em1/em1}) mice through the use of CRISPR-Cas9 technology. Two guide RNAs targeting the regions near the start and stop codons were used to delete the entire coding region of *Dnah8* (Figure S4A). Polymerase chain reaction (PCR) and Sanger sequencing were performed to confirm the mutated allele in *Dnah8*-KO mice (Figures S4B and S4C). We also used an immunoblot assay to investigate the level of DNAH8 protein in the testes of wild-type and *Dnah8*-KO male mice. As shown in Figure S5, the signal of DNAH8 was absent in the testes from *Dnah8*-KO male mice. No significant

differences were observed in testis weight between *Dnah8*-KO and heterozygous mutated male mice (Figure S6). Sperm parameters and morphology of *Dnah8*-KO male mice were also investigated. As shown in Table 3, Video S1, and Video S2, diminished sperm movement was

the sperm flagella from all three subjects harboring bi-allelic *DNAH8* variants, including both missense and frameshift variants (Figure 4A and Figure S3A). We also examined the presence of DNAH17, which is required for accurate localization of DNAH8.¹³ Notably, the staining

differences were observed in testis weight between *Dnah8*-KO and heterozygous mutated male mice (Figure S6). Sperm parameters and morphology of *Dnah8*-KO male mice were also investigated. As shown in Table 3, Video S1, and Video S2, diminished sperm movement was

Table 3. Sperm Characteristics and Flagellar Morphology of *Dnah8*-KO Male Mice

	Heterozygous Control (<i>Dnah8</i> ^{wt/em1})	KO (<i>Dnah8</i> ^{em1/em1})
Semen Parameter		
Motility (%)	91.7 ± 1.5	0 ± 0***
Sperm Flagellar Morphology^a		
Absent flagella (%)	4.0 ± 2.6	18.5 ± 17.8*
Short flagella (%)	0.0 ± 0.0	25.7 ± 1.2***
Coiled flagella (%)	0.0 ± 0.0	25.5 ± 15.6**
Irregular caliber (%)	0.2 ± 0.3	20.5 ± 12.6***
Bent flagella (%)	0.7 ± 0.8	9.8 ± 1.6***

^aData represent the mean ± SD of three independent experiments.
*p < 0.05, **p < 0.01, ***p < 0.001.

observed in *Dnah8*-KO male mice when compared to heterozygous mutated (*Dnah8*^{wt/em1}) male mice. H&E staining revealed significantly higher rates of abnormal flagella in *Dnah8*-KO male mice than those in heterozygous mutated male mice (Table 3 and Figure 5A). The sperm flagella of *Dnah8*-KO male mice also presented with absent, short, coiled, bent, and/or irregular shapes, which recapitulated the clinical phenotypes of MMAF-affected men with bi-allelic *DNAH8* variants. Furthermore, TEM analysis of sperm flagella showed disorganized microtubules and outer dense fibers in the spermatozoa from *Dnah8*-KO male mice (Figure 5B). These experimental observations on *Dnah8*-KO male mice conclusively demonstrated the crucial role of *DNAH8* in sperm flagellar formation.

To further investigate the role of *DNAH8* in spermatogenesis, we performed H&E staining on the testes of *Dnah8*-KO and heterozygous mutated male mice (Figure 6A). In stage VII–VIII seminiferous tubules, no elongated tails were observed in the testes from *Dnah8*-KO male mice, but normal round spermatids were observed, indicating the involvement of *DNAH8* in sperm flagellar formation. Periodic acid–Schiff (PAS) staining of the cauda epididymis from *Dnah8*-KO male mice displayed fewer sperm heads than did those from heterozygous mutated mice (Figure 6B). Collectively, these data suggest that *DNAH8* deficiency can result in MMAF and male infertility in both humans and mice.

To assess the fertility and reproductive behavior of *Dnah8*-KO male mice, sexually mature *Dnah8*-KO and heterozygous mutated male mice were individually caged with 8-week-old wild-type B6D2F1 female mice (one male with three females) for 2 months, and plugs were checked every morning. Pups were counted on the day of birth. As shown in Figure S7, normal mounting and copulatory plugs were observed for both groups of *Dnah8*-KO and heterozygous mutated male mice. However, *Dnah8*-KO male mice failed to produce any offspring over 2 months of breeding, whereas heterozygous mutated males routinely produced offspring (Figure S7). These

experimental observations indicate that *DNAH8* is necessary for male fertility in mice.

Intracytoplasmic sperm injection (ICSI) has been reported to be efficient for most MMAF-associated asthenoteratozoospermia.²³ To examine whether *DNAH8*-associated male infertility could also be overcome via ICSI, we conducted experiments using the sperm from wild-type and *Dnah8*-KO male mice. As shown in Figure 7, pups were successfully obtained upon ICSI using the spermatozoa from *Dnah8*-KO male mice after the transfer of two-cell embryos to pseudopregnant ICR females. Genotyping assays confirmed that all these pups were heterozygous *Dnah8*-mutated carriers, as anticipated. Our findings indicated that *Dnah8*-associated KO male infertility in mice could be overcome by ICSI. Consistent with these experimental observations, the second ICSI attempt performed using the sperm from subject F0300 (who harbored a homozygous *DNAH8* frameshift variant) was successful and resulted in a live birth. Overall, our data strongly suggest that ICSI could serve as a promising treatment for infertile men harboring bi-allelic *DNAH8* variants.

As highly conserved beating organelles, motile cilia and flagella are required for cell motility and signaling.²⁴ The axonemal ultrastructure, which is shared by cilia and flagella, consists of a circle of nine peripheral microtubule doublets arranged around a central pair of microtubules.¹⁷ Distinct multi-protein dynein complexes, which are attached regularly to peripheral microtubule doublets, contain molecular motors that can generate microtubule sliding and thus regulate the movement of motile cilia and flagella.¹⁹

The mammalian ODA is a complex structure that is attached to the peripheral microtubules via a docking complex. It is responsible for ciliary and flagellar beating.^{25–27} Previous studies reported two types of human ODAs. In airway epithelial cells, type 1 ODAs (e.g., *DNAH11*) reside in the proximal part of the cilium, whereas type 2 ODAs (e.g., *DNAH9*) reside in the distal part of the cilium.^{28,29} The deficiency of ODA-associated proteins results in PCD and/or asthenoteratozoospermia. For example, disruptions in *DNAH5* and *DNAH11* are associated with PCD.^{28,30} Furthermore, mutations in *DNAH9* (MIM: 603330), *DNAI1* (MIM: 604366), and *DNAI2* (MIM: 605483) induce PCD and male infertility.^{18,31,32} These previous observations indicate the important roles of ODA-associated proteins in ciliary and flagellar morphology and motility.

Here, our genetic analyses using WES on two distinct cohorts with MMAF (in total, 257 cases) identified three (1.2%) unrelated men carrying bi-allelic variants in *DNAH8*, which encodes an ODA heavy chain component of the axoneme that is preferentially expressed in the testis. These *DNAH8* variants are either rare or absent in human populations, but they were enriched in the MMAF-affected cases of different ancestries, indicating that *DNAH8* deficiency could be another important cause of MMAF across human populations.

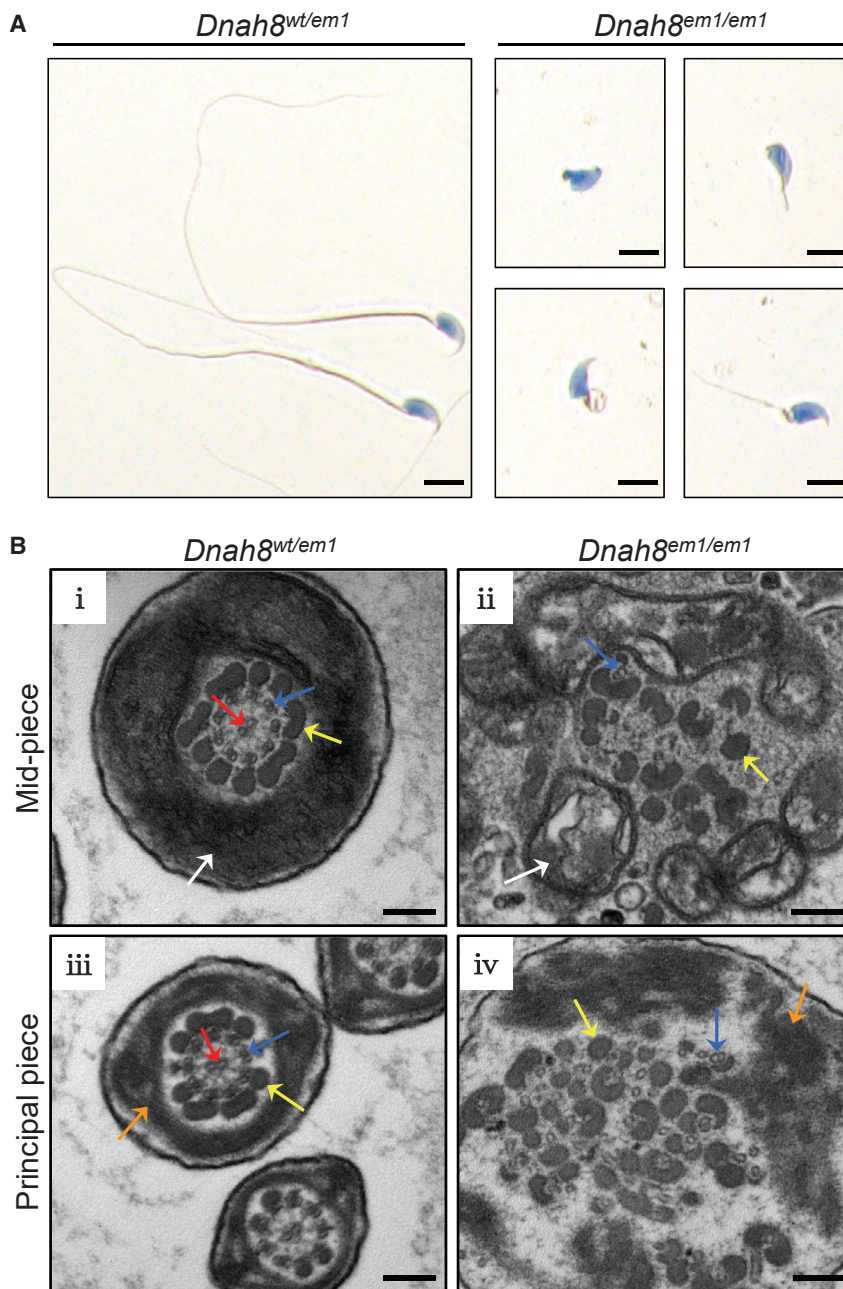


Figure 5. Sperm Morphology and Ultrastructure Analyses for *Dnah8*-KO Male Mice
 (A) H&E staining of the spermatozoa obtained from mouse cauda epididymis. The spermatozoa from heterozygous mutated (*Dnah8*^{wt/em1}) male mice showed normal morphology. In contrast, *Dnah8*-KO (*Dnah8*^{em1/em1}) male mice manifested aberrant flagellar morphologies, which were consistent with the clinical phenotypes in the MMAF-affected men. Scale bar: 5 μ m.
 (B) TEM of cross-sections of the spermatozoa from *Dnah8*-KO male mice. Cross-sections of the mid-piece (i) and principal piece (iii) of the sperm flagella in heterozygous mutated male mice are shown as controls. (ii) Cross-sections of the mid-piece of the sperm flagella in *Dnah8*-KO male mice revealed disorganization of mitochondrial sheaths, outer dense fibers, and microtubules. (iv) Cross-sections of the principal piece of the sperm flagella in *Dnah8*-KO male mice showed disorganization of fibrous sheaths, outer dense fibers, and microtubules. White arrows indicate mitochondrial sheath, orange arrows indicate fibrous sheaths, yellow arrows indicate outer dense fibers, blue arrows indicate peripheral microtubule doublets, and red arrows indicate the central pair of microtubules. Scale bars: 200 nm.

mRNA in the spermatozoa from subject A051 harboring bi-allelic *DNAH8* missense variants was significantly reduced (Figure S2). This may be due to the recognition of specific sets of mutated mRNAs by RNA-binding proteins, which serve as adaptors and control decay rates by recruitment of RNA-degrading enzymes.³⁴ The reduced mRNA abundance in low-motility sperm was also previously observed for other members (such as *DNAH1* and *DNAH7*) of the axonemal dynein family.³⁵

Further phenotypic analysis revealed that men harboring bi-allelic *DNAH8* variants displayed typical MMAF phenotypes, including reduced sperm motility, missing microtubule doublets, and disassembled or absent ODAs. Intriguingly, ODAs were still present in small amounts on observable doublets in the sperm flagella from subject A051 (who harbored bi-allelic *DNAH8* missense variants), whereas ODAs were absent from those of subject F0300 (who harbored a homozygous frameshift variant of *DNAH8*). This phenomenon may be due to a possible phenotype continuum depending on the severity of variants in MMAF-associated genes, as previously shown for *CFAP70*, *DNAH1*, and *DNAH17*.^{2,13,20,33}

Functional experiments further revealed the pathogenicity of bi-allelic *DNAH8* variants. The level of *DNAH8*

The remaining mutated mRNA of *DNAH8* may produce a small amount of mis-folded DNAH8 protein. However, the immunostaining of DNAH8 was almost absent in the sperm flagella from men harboring bi-allelic *DNAH8* variants. This near absence of DNAH8 protein may result from specific degradation of unfolded proteins by the “unfolded protein response” described in previous studies.^{36,37}

A previous study described the absence of DNAH8 protein in the spermatozoa from men harboring bi-allelic *DNAH17* variants.¹³ The present investigations on the amount and localization of DNAH17 revealed a dramatic reduction of DNAH17 in the sperm cells from men harboring bi-allelic *DNAH8* variants. These observations confirm the interaction between DNAH8 and DNAH17 during spermatogenesis. Several previous studies also reported that DNAH8

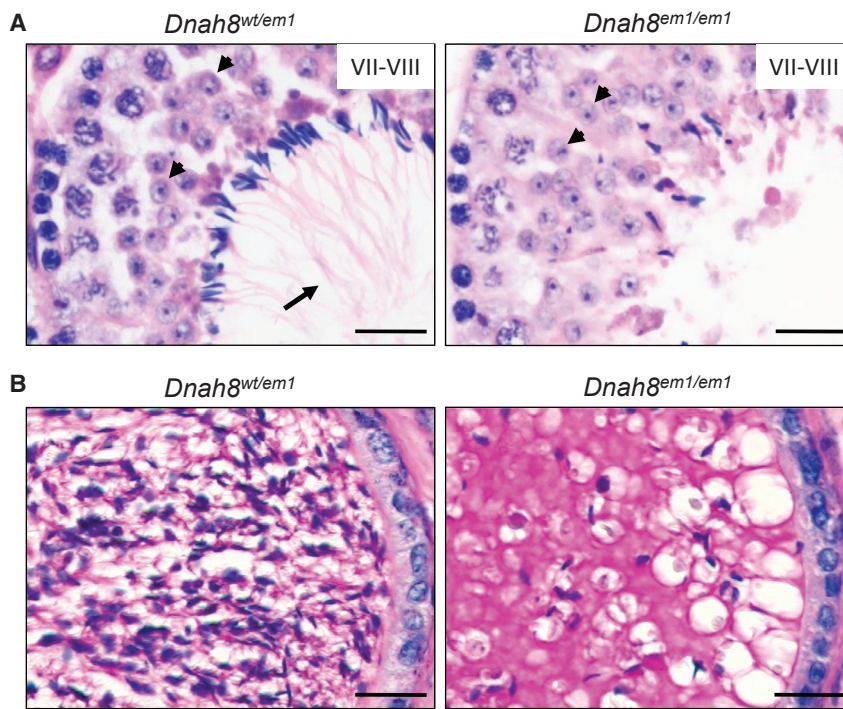


Figure 6. *Dnah8* is Essential for Normal Spermatogenesis in Mice

(A) The development of sperm flagella was investigated in mouse testis through the use of H&E staining. In stage VII–VIII seminiferous tubules, normal round spermatids (arrowheads) were observed, but elongated tails (arrows) were not observed in the testes from *Dnah8*-KO (*Dnah8*^{em1/em1}) male mice. Scale bar: 20 μ m.

(B) PAS staining of the cauda epididymis from male mice. Decreased sperm quantity was observed in the epididymis from *Dnah8*-KO male mice, when compared with that in heterozygous mutated (*Dnah8*^{wt/em1}) male mice. Scale bar: 20 μ m.

and DNAH17 were categorically detectable in human sperm proteome analyses.^{38,39} DNAH17 is required for flagellar biogenesis and stabilization of microtubule doublets 4–7.²⁰ Our TEM analysis of sperm also indicated a destabilization of microtubule doublets 4–7 in the principal piece of spermatozoa from men harboring bi-allelic *DNAH8* variants. This characteristic defect shared by DNAH8-associated and DNAH17-associated cases further suggests that DNAH8 and DNAH17 proteins are dependent on each other during flagellar assembly and spermatogenesis.

Presently, *Dnah8*-KO male mice displayed MMAF phenotypes, including diminished sperm motility and abnormal flagella. Furthermore, H&E and PAS staining analyses revealed abnormal spermatogenesis in the testis and reduced sperm counts in the cauda epididymis from *Dnah8*-KO male mice. Previous studies showed that ODAs are preassembled in the cell body and transported as a holo-complex into the cilium, where they dock to the axonemal microtubules via intraflagellar transport (IFT).^{40–43} These observations further indicate the important role of ODAs in cell differentiation. Similar results were also found in the spermatozoa with defects in IDA-associated proteins. For example, the spermatozoa from men with *DNAH1* mutations showed severely disarranged axonemal structures with loss of IDAs.² All these observations indicate that mutations in dynein proteins not only induce the lack of ODAs and IDAs, but also affect assembly of the axoneme. Therefore, structural abnormalities in the sperm axoneme from men harboring bi-allelic *DNAH8* variants and *Dnah8*-KO male mice are likely caused by the flagellar assembly defects during spermatogenesis. Notably, the decreased sperm counts in *Dnah8*-KO male mice were not observed in men harboring bi-allelic *DNAH8* variants, and this

may potentially reflect evolutionarily divergent protein regulatory networks of DNAH8 between human and mouse.

As an assisted reproductive technology, ICSI has been regarded as an effective way to help infertile couples achieve a successful pregnancy. Previous studies have suggested that MMAF-affected men harboring *DNAH1* variants could acquire good prognoses following ICSI, with 70.8% overall fertilization, 50.0% pregnancy, and 37.5% delivery rates.⁴⁴ In contrast, ICSI has been reported to fail for the MMAF-affected men carrying *CEP135* (MIM: 611423) or *DNAH17* variants.^{13,45} In this study, ICSI experiments were performed using the sperm from *Dnah8*-KO male mice. Although the rate of two-cell embryos in the *Dnah8*-KO group was lower than that of the wild-type control group, we obtained healthy pups, indicating a successful ICSI treatment in the *Dnah8*-KO mouse model. Furthermore, ICSI was also successful for human subject F0300 and resulted in a positive pregnancy outcome and a live birth. Therefore, our findings indicate that ICSI can be recommended for *DNAH8*-associated asthenoteratozoospermia.

In conclusion, we identified *DNAH8* as an asthenoteratozoospermia-associated gene in both humans and mice. The observed effects of DNAH8 deficiency on DNAH17 localization in the sperm flagella further suggested that dynein-arms-associated proteins may affect spermatogenesis in a collaborative manner. Furthermore, *DNAH8*-associated MMAF and male infertility could be treated through the use of ICSI. Our findings will be informative for genetic and reproductive counseling of infertile men with asthenoteratozoospermia.

Data and Code Availability

The NCBI reference sequence number for *DNAH8* transcript is NM_001206927.2. The NCBI reference sequence number for DNAH8 protein is NP_001193856.1.

A

Males providing sperm	No. of oocytes injected	No. of 2-cell embryos	No. of pups delivered
<i>Dnah8^{wt/wt}</i>	44	15	2
<i>Dnah8^{em1/em1}</i>	81	14	3

B



C

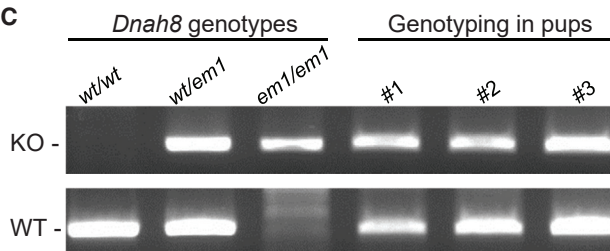


Figure 7. Pups Obtained upon ICSI using the Spermatozoa from *Dnah8*-KO Male Mice

(A) Development of ICSI embryos. Fourteen (17.3%) of the 81 oocytes injected with the spermatozoa from *Dnah8*-KO (*Dnah8^{em1/em1}*) male mice developed to the two-cell stage, and three pups were obtained after embryo transfer. ICSI data from the use of sperm from wild-type male mice are shown as controls. (B) The pups obtained from ICSI using the spermatozoa from *Dnah8*-KO male mice.

(C) Genotyping of these pups. All of the pups carried the heterozygous *Dnah8*-mutated allele. KO denotes the mutated allele and WT denotes the wild-type allele.

Supplemental Data

Supplemental Data can be found online at <https://doi.org/10.1016/j.ajhg.2020.06.004>.

Acknowledgments

We would like to thank the families for participating and supporting this study. We also thank the Center of Cryo-electron Microscopy at Zhejiang University, the transmission electron microscopy core facility of the Institut Cochin (INSERM U1016, Paris), and Yonggang Lu at Osaka University for technical support. This work was supported by the Ministry of Education, Culture, Sports, Science and Technology (MEXT)/Japan Society for the Promotion of Science (JSPS) (KAKENHI grants JP17H04987 to H.M. and JP19H05750 to M.I.), the National Natural Science Foundation of China (31625015, 31521003, 81901541, 81971441, and 81871200), the Eunice Kennedy Shriver National Institute of Child Health and Human Development (P01HD087157 and R01HD088412 to M.I.), the Bill and Melinda Gates Foundation (INV-001902 to M.I.), the Institut National de la Santé et de la

Recherche Médicale (Inserm), the Centre National de la Recherche Scientifique (CNRS), the Université de Paris and the French National Research Agency (MASFLAGELLA ANR-14-CE15-0002 and FLAGEL-OME ANR18-CE17-0014 to P.F.R. and A.T.), Shanghai Medical Center of Key Programs for Female Reproductive Diseases (2017ZZ01016), and Shanghai Municipal Science and Technology Major Project (2017SHZDZX01).

Declaration of Interests

The authors declare no competing interests.

Received: March 19, 2020

Accepted: June 5, 2020

Published: July 2, 2020

Web Resources

1000 Genomes Project, <https://www.internationalgenome.org>
 gnomAD, <https://gnomad.broadinstitute.org>
 HUGO Gene Nomenclature Committee, <https://www.genenames.org>
 Human Protein Atlas, <https://www.proteinatlas.org>
 National Center for Biotechnology Information (NCBI), <https://www.ncbi.nlm.nih.gov/>
 Online Mendelian Inheritance in Man, <https://www.omim.org>
 PolyPhen-2, <http://genetics.bwh.harvard.edu/pph2/>
 SIFT, <https://sift.bii.a-star.edu.sg>
 UniProt, <https://www.uniprot.org>

References

- Hosseini, B., Nourmohamadi, M., Hajipour, S., Taghizadeh, M., Asemi, Z., Keshavarz, S.A., and Jafarnejad, S. (2019). The Effect of Omega-3 Fatty Acids, EPA, and/or DHA on Male Infertility: A Systematic Review and Meta-analysis. *J. Diet. Suppl.* *16*, 245–256.
- Ben Khelifa, M., Coutton, C., Zouari, R., Karaouzen, T., Rendu, J., Bidart, M., Yassine, S., Pierre, V., Delaroche, J., Hennebicq, S., et al. (2014). Mutations in DNAH1, which encodes an inner arm heavy chain dynein, lead to male infertility from multiple morphological abnormalities of the sperm flagella. *Am. J. Hum. Genet.* *94*, 95–104.
- Baccetti, B., Collodel, G., Estenoz, M., Manca, D., Moretti, E., and Piomboni, P. (2005). Gene deletions in an infertile man with sperm fibrous sheath dysplasia. *Hum. Reprod.* *20*, 2790–2794.
- Tang, S., Wang, X., Li, W., Yang, X., Li, Z., Liu, W., Li, C., Zhu, Z., Wang, L., Wang, J., et al. (2017). Biallelic Mutations in CFAP43 and CFAP44 Cause Male Infertility with Multiple Morphological Abnormalities of the Sperm Flagella. *Am. J. Hum. Genet.* *100*, 854–864.
- Dong, F.N., Amiri-Yekta, A., Martinez, G., Saut, A., Tek, J., Stouvenel, L., Lorès, P., Karaouzen, T., Thierry-Mieg, N., Satre, V., et al. (2018). Absence of CFAP69 Causes Male Infertility due to Multiple Morphological Abnormalities of the Flagella in Human and Mouse. *Am. J. Hum. Genet.* *102*, 636–648.
- Kherraf, Z.E., Amiri-Yekta, A., Dacheux, D., Karaouzen, T., Coutton, C., Christou-Kent, M., Martinez, G., Landrein, N., Le Tanno, P., Fourati Ben Mustapha, S., et al. (2018). A Homozygous Ancestral SVA-Insertion-Mediated Deletion in WDR66

- Induces Multiple Morphological Abnormalities of the Sperm Flagellum and Male Infertility. *Am. J. Hum. Genet.* *103*, 400–412.
7. Auguste, Y., Delague, V., Desvignes, J.P., Longepied, G., Gnisci, A., Besnier, P., Levy, N., Beroud, C., Megarbane, A., Metzler-Guillemain, C., and Mitchell, M.J. (2018). Loss of Calmodulin- and Radial-Spoke-Associated Complex Protein CFAP251 Leads to Immotile Spermatozoa Lacking Mitochondria and Infertility in Men. *Am. J. Hum. Genet.* *103*, 413–420.
 8. Coutton, C., Martinez, G., Kherraf, Z.E., Amiri-Yekta, A., Boguenet, M., Saut, A., He, X., Zhang, F., Cristou-Kent, M., Escoffier, J., et al. (2019). Bi-allelic Mutations in *ARMC2* Lead to Severe Astheno-Teratozoospermia Due to Sperm Flagellum Malformations in Humans and Mice. *Am. J. Hum. Genet.* *104*, 331–340.
 9. Liu, W., He, X., Yang, S., Zouari, R., Wang, J., Wu, H., Kherraf, Z.E., Liu, C., Coutton, C., Zhao, R., et al. (2019). Bi-allelic Mutations in *TTC21A* Induce Asthenoteratospermia in Humans and Mice. *Am. J. Hum. Genet.* *104*, 738–748.
 10. Coutton, C., Vargas, A.S., Amiri-Yekta, A., Kherraf, Z.E., Ben Mustapha, S.F., Le Tanno, P., Wambergue-Legrand, C., Karaouzen, T., Martinez, G., Crouzy, S., et al. (2018). Mutations in *CFAP43* and *CFAP44* cause male infertility and flagellum defects in *Trypanosoma* and human. *Nat. Commun.* *9*, 686.
 11. Liu, C., He, X., Liu, W., Yang, S., Wang, L., Li, W., Wu, H., Tang, S., Ni, X., Wang, J., et al. (2019). Bi-allelic Mutations in *TTC29* Cause Male Subfertility with Asthenoteratospermia in Humans and Mice. *Am. J. Hum. Genet.* *105*, 1168–1181.
 12. Lorès, P., Dacheux, D., Kherraf, Z.E., Nsota Mbango, J.F., Coutton, C., Stouvenel, L., Ialy-Radio, C., Amiri-Yekta, A., Whitfield, M., Schmitt, A., et al. (2019). Mutations in *TTC29*, Encoding an Evolutionarily Conserved Axonemal Protein, Result in Asthenozoospermia and Male Infertility. *Am. J. Hum. Genet.* *105*, 1148–1167.
 13. Whitfield, M., Thomas, L., Bequignon, E., Schmitt, A., Stouvenel, L., Montantin, G., Tissier, S., Duquesnoy, P., Copin, B., Chantot, S., et al. (2019). Mutations in *DNAH17*, Encoding a Sperm-Specific Axonemal Outer Dynein Arm Heavy Chain, Cause Isolated Male Infertility Due to Asthenozoospermia. *Am. J. Hum. Genet.* *105*, 198–212.
 14. Touré, A., Martinez, G., Kherraf, Z.E., Cazin, C., Beurois, J., Arnoult, C., Ray, P.F., and Coutton, C. (2020). The genetic architecture of morphological abnormalities of the sperm tail. *Hum. Genet.* <https://doi.org/10.1007/s00439-00020-02113-x>.
 15. Reiter, J.E., and Leroux, M.R. (2017). Genes and molecular pathways underpinning ciliopathies. *Nat. Rev. Mol. Cell Biol.* *18*, 533–547.
 16. Zariwala, M.A., Knowles, M.R., and Omran, H. (2007). Genetic defects in ciliary structure and function. *Annu. Rev. Physiol.* *69*, 423–450.
 17. Ishikawa, T. (2017). Axoneme Structure from Motile Cilia. *Cold Spring Harb. Perspect. Biol.* *9*, a028076.
 18. Loges, N.T., Olbrich, H., Fenske, L., Mussaffi, H., Horvath, J., Fliegauf, M., Kuhl, H., Baktai, G., Peterffy, E., Chodhari, R., et al. (2008). *DNAI2* mutations cause primary ciliary dyskinesia with defects in the outer dynein arm. *Am. J. Hum. Genet.* *83*, 547–558.
 19. Ibañez-Tallon, I., Heintz, N., and Omran, H. (2003). To beat or not to beat: roles of cilia in development and disease. *Hum. Mol. Genet.* *12*, R27–R35.
 20. Zhang, B., Ma, H., Khan, T., Ma, A., Li, T., Zhang, H., Gao, J., Zhou, J., Li, Y., Yu, C., et al. (2020). A *DNAH17* missense variant causes flagella destabilization and asthenozoospermia. *J. Exp. Med.* *217*, e20182365.
 21. Wang, Y., Yang, J., Jia, Y., Xiong, C., Meng, T., Guan, H., Xia, W., Ding, M., and Yuchi, M. (2014). Variability in the morphologic assessment of human sperm: use of the strict criteria recommended by the World Health Organization in 2010. *Fertil. Steril.* *101*, 945–949.
 22. Samant, S.A., Ogunkua, O.O., Hui, L., Lu, J., Han, Y., Orth, J.M., and Pilder, S.H. (2005). The mouse t complex distorter/sterility candidate, *Dnahc8*, expresses a gamma-type axonemal dynein heavy chain isoform confined to the principal piece of the sperm tail. *Dev. Biol.* *285*, 57–69.
 23. Chemes, H.E., and Alvarez Sedo, C. (2012). Tales of the tail and sperm head aches: changing concepts on the prognostic significance of sperm pathologies affecting the head, neck and tail. *Asian J. Androl.* *14*, 14–23.
 24. Viswanadha, R., Sale, W.S., and Porter, M.E. (2017). Ciliary Motility: Regulation of Axonemal Dynein Motors. *Cold Spring Harb. Perspect. Biol.* *9*, a018325.
 25. Loges, N.T., Antony, D., Maver, A., Deardorff, M.A., Güleç, E.Y., Gezdirici, A., Nöthe-Menchen, T., Höben, I.M., Jelten, L., Frank, D., et al. (2018). Recessive *DNAH9* Loss-of-Function Mutations Cause Laterality Defects and Subtle Respiratory Ciliary-Beating Defects. *Am. J. Hum. Genet.* *103*, 995–1008.
 26. King, S.M. (2016). Axonemal Dynein Arms. *Cold Spring Harb. Perspect. Biol.* *8*, a028100.
 27. Pazour, G.J., Agrin, N., Walker, B.L., and Witman, G.B. (2006). Identification of predicted human outer dynein arm genes: candidates for primary ciliary dyskinesia genes. *J. Med. Genet.* *43*, 62–73.
 28. Fliegauf, M., Olbrich, H., Horvath, J., Wildhaber, J.H., Zariwala, M.A., Kennedy, M., Knowles, M.R., and Omran, H. (2005). Mislocalization of *DNAH5* and *DNAH9* in respiratory cells from patients with primary ciliary dyskinesia. *Am. J. Respir. Crit. Care Med.* *171*, 1343–1349.
 29. Dougherty, G.W., Loges, N.T., Klinckenbusch, J.A., Olbrich, H., Pennekamp, P., Menchen, T., Raidt, J., Wallmeier, J., Werner, C., Westermann, C., et al. (2016). *DNAH11* Localization in the Proximal Region of Respiratory Cilia Defines Distinct Outer Dynein Arm Complexes. *Am. J. Respir. Cell Mol. Biol.* *55*, 213–224.
 30. Liu, S., Chen, W., Zhan, Y., Li, S., Ma, X., Ma, D., Sheng, W., and Huang, G. (2019). *DNAH11* variants and its association with congenital heart disease and heterotaxy syndrome. *Sci. Rep.* *9*, 6683.
 31. Guichard, C., Harricane, M.C., Lafitte, J.J., Godard, P., Zaegel, M., Tack, V., Lalau, G., and Bouvagnet, P. (2001). Axonemal dynein intermediate-chain gene (*DNAI1*) mutations result in situs inversus and primary ciliary dyskinesia (Kartagener syndrome). *Am. J. Hum. Genet.* *68*, 1030–1035.
 32. Fassad, M.R., Shoemark, A., Legendre, M., Hirst, R.A., Koll, F., le Borgne, P., Louis, B., Daudvohra, F., Patel, M.P., Thomas, L., et al. (2018). Mutations in Outer Dynein Arm Heavy Chain *DNAH9* Cause Motile Cilia Defects and Situs Inversus. *Am. J. Hum. Genet.* *103*, 984–994.
 33. Beurois, J., Martinez, G., Cazin, C., Kherraf, Z.E., Amiri-Yekta, A., Thierry-Mieg, N., Bidart, M., Petre, G., Satre, V., Brouillet, S., et al. (2019). *CFAP70* mutations lead to male infertility due to severe astheno-teratozoospermia. A case report. *Hum. Reprod.* *34*, 2071–2079.

34. Stoecklin, G., and Mühlemann, O. (2013). RNA decay mechanisms: specificity through diversity. *Biochim. Biophys. Acta* 1829, 487–490.
35. Caballero-Campo, P., Lira-Albarrán, S., Barrera, D., Borja-Cacho, E., Godoy-Morales, H.S., Rangel-Escareño, C., Larrea, F., and Chirinos, M. (2020). Gene transcription profiling of astheno- and normo-zoospermic sperm subpopulations. *Asian J. Androl.* 22. https://doi.org/10.4103/aja.aja_4143_4119.
36. Rutkowski, D.T., and Hegde, R.S. (2010). Regulation of basal cellular physiology by the homeostatic unfolded protein response. *J. Cell Biol.* 189, 783–794.
37. Wang, S., and Kaufman, R.J. (2012). The impact of the unfolded protein response on human disease. *J. Cell Biol.* 197, 857–867.
38. Wang, G., Guo, Y., Zhou, T., Shi, X., Yu, J., Yang, Y., Wu, Y., Wang, J., Liu, M., Chen, X., et al. (2013). In-depth proteomic analysis of the human sperm reveals complex protein compositions. *J. Proteomics* 79, 114–122.
39. Amaral, A., Castillo, J., Estanyol, J.M., Ballescà, J.L., Ramalho-Santos, J., and Oliva, R. (2013). Human sperm tail proteome suggests new endogenous metabolic pathways. *Mol. Cell. Proteomics* 12, 330–342.
40. Fowkes, M.E., and Mitchell, D.R. (1998). The role of preassembled cytoplasmic complexes in assembly of flagellar dynein subunits. *Mol. Biol. Cell* 9, 2337–2347.
41. Dean, A.B., and Mitchell, D.R. (2013). *Chlamydomonas* ODA10 is a conserved axonemal protein that plays a unique role in outer dynein arm assembly. *Mol. Biol. Cell* 24, 3689–3696.
42. Dean, A.B., and Mitchell, D.R. (2015). Late steps in cytoplasmic maturation of assembly-competent axonemal outer arm dynein in *Chlamydomonas* require interaction of ODA5 and ODA10 in a complex. *Mol. Biol. Cell* 26, 3596–3605.
43. Desai, P.B., Freshour, J.R., and Mitchell, D.R. (2015). *Chlamydomonas* axonemal dynein assembly locus ODA8 encodes a conserved flagellar protein needed for cytoplasmic maturation of outer dynein arm complexes. *Cytoskeleton (Hoboken)* 72, 16–28.
44. Wambergue, C., Zouari, R., Fourati Ben Mustapha, S., Martinez, G., Devillard, F., Hennebicq, S., Satre, V., Brouillet, S., Halouani, L., Marrakchi, O., et al. (2016). Patients with multiple morphological abnormalities of the sperm flagella due to DNAH1 mutations have a good prognosis following intracytoplasmic sperm injection. *Hum. Reprod.* 31, 1164–1172.
45. Sha, Y.W., Xu, X., Mei, L.B., Li, P., Su, Z.Y., He, X.Q., and Li, L. (2017). A homozygous CEP135 mutation is associated with multiple morphological abnormalities of the sperm flagella (MMAF). *Gene* 633, 48–53.
46. Cooper, T.G., Noonan, E., von Eckardstein, S., Auger, J., Baker, H.W., Behre, H.M., Haugen, T.B., Kruger, T., Wang, C., Mbizvo, M.T., and Vogelsong, K.M. (2010). World Health Organization reference values for human semen characteristics. *Hum. Reprod. Update* 16, 231–245.
47. Auger, J., Jouannet, P., and Eustache, F. (2016). Another look at human sperm morphology. *Hum. Reprod.* 31, 10–23.